PAPER

Check for updates

Self-assembled sonogels formed from 1,4-naphthalenedicarbonyldinicotinic acid hydrazide†

Lieqiang Liao, ‡ Ruidong Liu, ‡ Shuwen Hu, Wenting Jiang, Yali Chen, Jinlian Zhong, Xinjian Jia, * Huijin Liu * and Xuzhong Luo *

In this paper, we report self-assembled sonogels formed from 1,4-naphthalenedicarbonyldinicotinic acid hydrazide (NDC-NN3) in some liquids including ethanol, tetrahydrofuran (THF), 1,4-dioxane, n-propanol, n-butanol and n-pentanol. When the clear solution of NDC-NN3 in the selected liquids mentioned above at a suitable concentration was irradiated with ultrasound waves at room temperature, a sonogel was formed. Upon heating, the sonogel dissolved gradually and finally became a clear solution again. Upon cooling the hot solution to room temperature, the solution state did not change even after standing for a few days. Nevertheless, if the solution underwent sonication for a certain time, a stable gel was obtained again. The critical gelation concentrations (CGCs) of NDC-NN3 in ethanol, THF, 1,4-dioxane, n-propanol, n-butanol and n-pentanol are 10, 8, 6, 8, 6 and 8 mg mL^{-1}, respectively. The obtained sonogels display excellent mechanical properties. The crystal structure of NDC-NN3 suggests that the naphthalene ring, hydrazide group and the position of N in the pyridine ring mediate the self-assembly process. Upon sonication, the formation of suitable $\pi-\pi$ stacking and intermolecular hydrogen bonding drives the gelator molecules to self-assemble into fibers, spheres and micro-burdock-shaped balls in various solvents, which ultimately confine the liquids.

1. Introduction

Stimuli-responsive smart materials have attracted wide attention because of their potential applications in catalysis, controlled release drug delivery, biosensing, tissue engineering, and so on.[1] Supramolecular gels are ideal candidates for soft, stimuli-responsive materials because the modifiable molecular structures of gelators endow them with sensitivity to pH, light, solvents and guest molecules. To date, although a large number of low molecular-weight gels based on hydrogen bonding, metal–ligand coordination, aromatic interactions, van der Waals forces and hydrophobic effects have been reported,[2] how to design and prepare a low molecular-weight gel with specific properties is still a challenge.

It has been known that external stimuli, such as temperature, pH, light, mechanical stress, solvent or additives, can

induce sol–gel transitions by modulating the gel-forming interactions.[3] Following the pioneering research by Naota and Koori,[4] some sonogelators with the chemical structure including organometallics,[5] peptides,[6] ureas,[7] cholesterols[8] and heterocycles[9] have been synthesized. These sonogels have potential applications such as wettability switches, hybrid materials, pollutant decontaminants or cell encapsulators.[10] Previous reports reveal that hydrazide derivatives presented in many bioactive molecules display a wide range of biological activities, including antibacterial, antifungal, anti-inflammatory, etc.[11] Although some organic compounds containing hydrazide groups can form supramolecular gels in previous reports,[12,13] the sonogelators derived from hydrazide are relatively few.[13]

In present article, we depict the ultrasound-treated gelation of a new simple acylhydrazine derivative gelator, 1,4-naphthalenedicarbonyldinicotinic acid hydrazide (NDC-NN3), in its clear solutions of ethanol, tetrahydrofuran, 1,4-dioxane, n-butanol and n-pentanol at room temperature. When a clear solution of NDC-NN3 in the selected liquids mentioned above at a suitable concentration was irradiated with ultrasound wave for a certain time at room temperature, a sonogel was formed. Upon heating, the sonogel dissolved gradually and finally became a clear solution. Cooling the hot solution to room temperature, only a clear solution obtained and no gelation was observed even standing the solution for a few days. After sonication for a certain time, stable gel was obtained again. The

morphology and microstructure of the corresponding xerogels, thermo-stability and reversible behavior of the sonogels and the relationship between gelation behavior and molecular structure were investigated. The self-assembled mechanism of the gelators in liquids was also be explored.

2. Experimental section

2.1 Materials

All materials employed in this paper were commercially available. Analytical grade 1,4-naphthalenedicarboxylic acid, nicotinic acid hydrazide, isonicotinic acid hydrazide, pyridine-2-carboxylic acid hydrazide, benzoic acid hydrazide, 3-aminopyridine, 4-aminopyridine and thionylchloride ($COCl_2$) were supplied by Aladdin Chemical Reagent Co., Ltd (Shanghai, China) and used without further purification. Analytical grade ethanol-d_6 and dimethyl sulfoxide-d_6 were purchased from J&K Scientific Co., Ltd (Shanghai, China). The solvents of triethylamine and dichloromethane (DCM) were distilled before use. All other solvents were obtained from Tianjin Damao Chemical Reagent Factory (Tianjin, China) and used without further purification.

2.2 Synthesis and gelation test

The compounds, 1,4-naphthalenedicarbonyldinicotinic acid hydrazide (NDC-NN3), 1,4-naphthalenedicarbonyldiisonicotinic acid hydrazide (NDC-NN4), 1,4-naphthalenedicarbonyldipyridine-2-carboxylic acid hydrazide (NDC-NN2), 1,4-naphthalenedicarbonyldibenzoic acid hydrazide (NDC-NNpH), N^1,N^4-di(pyridin-3-yl)-naphthalene-1,4-dicarboxamide (NDC-N3) and N^1,N^4-di(pyridin-4-yl)-naphthalene-1,4-dicarboxamide (NDC-N4) were synthesized by a typical amide condensation reaction. The detailed chemical structure, synthetic route and characterization were shown in Fig. 1a, Scheme S1 and Fig. S1–S4 (ESI).† The obtained compounds were characterized by FT-IR, ^{1}H NMR, ^{13}C NMR and LC-MS, respectively (Scheme S1, ESI†).

The 'inverted-vial test' method was used as a visual technique to test the sonication-induced gelation (sonogel) of NDC-NN3. Glass vials containing NDC-NN3 and solvents (1 mL) with different concentrations were heated for several minutes, and then cooled to room temperature to form clear solutions. Subsequently, the solutions were sonicated (40 KHz, 0.40 W cm^{-2}) in deionized water for a certain time at room temperature to promote complete sol–gel conversion. If the vial was turned upside down, in which the viscoelastic mixture that did not fall down could be defined as a gel.

2.3 Characterization

Morphology of xerogels was investigated on a FEI Quanta 450 scanning electron microscopy spectrometer (SEM). The accelerating voltage was 20 kV, and the spot was 3.0. The xerogels were obtained via vacuum freeze-drying (FD-1-50, Beijing Boyikang Experimental Instrument Co., Ltd) for 48 h. The Rheological experiments of sonogels were performed using a stress-controlled rheometer (HAAKE RheoStress 6000) with parallel
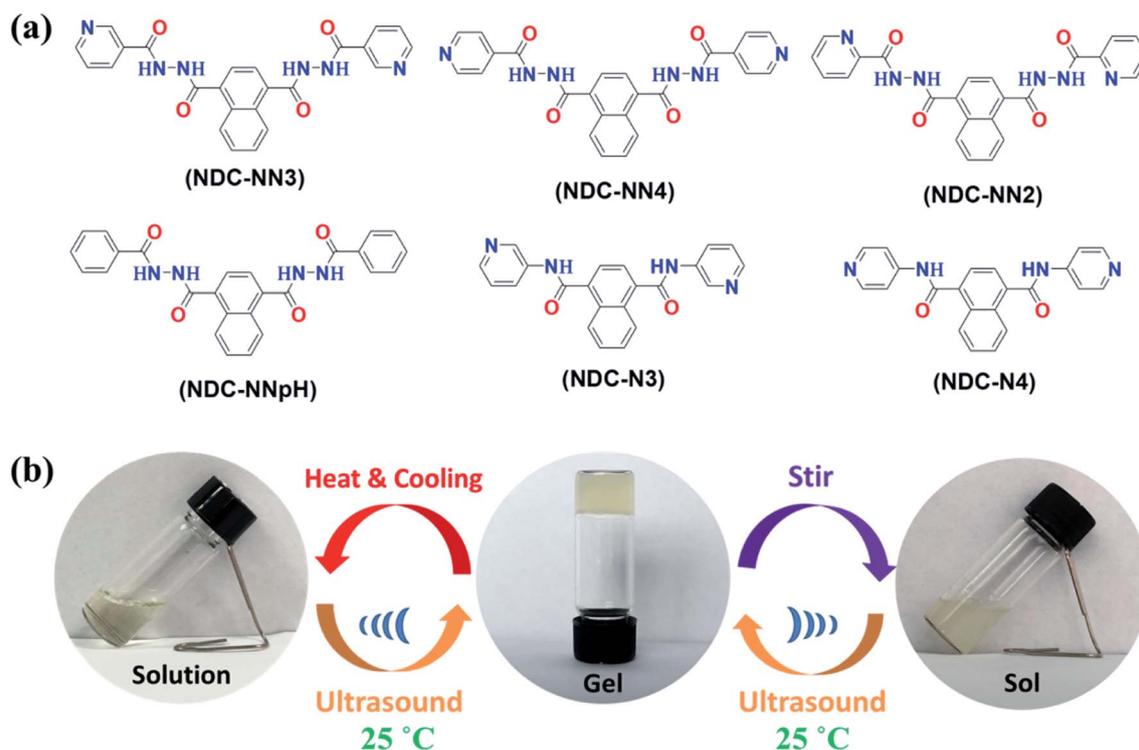

Fig. 1 (a) Chemical structures of the acylhydrazine and amide functionalized 1,4-naphthalenedicarboxylic acid derivatives reported in this work and (b) schematic diagram of the reversible sol–gel transformation for NDC-NN3 in ethanol upon various external stimuli.

plate type geometry (plate diameter, 3.5 cm). ^{1}H NMR and ^{13}C NMR spectra were acquired by using a Bruker AM 400 spectrometer. Small-angle X-ray powder diffraction (SA-XRD) patterns were taken with a Bruker D8 Focus diffractometer by using the Cu-$K\alpha$ radiation ($\lambda = 1.5418$ Å). Crystals suitable for X-ray diffraction studies were analyzed by using a Bruker Smart APEX II diffractometer. Fourier transform infrared (FT-IR) spectra were recorded in the region between 4000 and 400 cm^{-1} using KBr pellets and a Nicolet AVATAR 360 spectrometer. Mass spectra were recorded by using Shimadzu LCMS-9030. Samples were determined by HPLC by using a Waters e2695 HPLC model with a Waters 2998 PDA detector (MA, USA) operated at 236 nm, a 250 × 4.6 mm Phenomenex Gemini C18 was used, analyses were performed under isocratic conditions, the mobile phase consisting of methanol:H$_2$O (9 : 1, v/v) was eluted at 1 mL min^{-1}. Ultrasonic irradiation was performed using a KQ-600B ultrasonic bath (40 KHz, 0.40 W cm^{-2}).

3. Results and discussion

3.1 Gelation properties

The gelation properties of the as-obtained compounds were examined *via* a conventional heating-cooling process. It was found that none of the compounds tested in the experiment exhibited gelation ability in all tested solvents (Table S1 and S2, ESI†). Interestingly, when a clear solution of NDC-NN3 in ethanol (10 mg mL^{-1}) was irradiated with ultrasound wave (40 KHz, 0.40 W cm^{-2}) for a certain time at room temperature, a pale yellow opaque sonogel was formed. Upon heating, as shown in Fig. 1b, the sonogel of ethanol dissolved gradually and finally became a clear solution again. Cooling the hot solution to room temperature, only a clear solution was obtained and no gelation was observed even standing the solution for a few days. Nevertheless, if the solution underwent sonication for a certain time, stable gel obtained again. The ultrasonic duration needed for gel formation decreased with the increase of NDC-NN3 concentration in ethanol (Table S3, ESI†). For example, the ultrasonic durations needed for gelation of 10, 20 and 40 mg mL^{-1} of NDC-NN3 in ethanol were 60, 20 and 5 min, respectively. Intriguingly, if the sonogel was destroyed by mechanical stir (electro-magnetic stirring, the rate of stirring greater than 300 rpm), it would be recovery after sonication irradiation. The mechanism behind the responsiveness could be attributed to the modulation of the interactions between gelators and that between gelator and solvent molecules during ultrasonic irradiation, while the stirring breaks the balance of interactions.

Similar sonogelation was also exhibited in the NDC-NN3 solution of tetrahydrofuran, 1,4-dioxane, *n*-propanol, *n*-butanol or *n*-pentanol, while no sonogelation for methanol, ethylene glycol and some other organic mediums selected for the experiments (Table S1 and Fig. S5–S7, ESI†), implying that the gelling abilities of the sonogelators strongly depend on solvent properties. The critical gelation concentrations (CGC) of NDC-NN3 in ethanol, THF, 1,4-dioxane, *n*-propanol, *n*-butanol and *n*-pentanol are 10, 8, 6, 8, 6 and 8 mg mL^{-1} (1.27, 0.90, 0.58, 1.00, 0.74 and 0.98 wt%), respectively (Table S3 and Fig. S6, ESI†). These values are typical for supramolecular gels formed

by low-molecular-weight gelators.[2] Analyses (HPLC, ^{1}H NMR and ^{13}C NMR) of the gelator before and after ultrasound-induced gelation showed no degradation or chemical transformation in composition, confirming the supramolecular nature of the sonogelation process (Fig. S8–S10, ESI†).

Ethanol solutions with various water fraction (v/v = 5%, 8%, 10%) were used for gelation experiments, and the sonication induced gelation tests for the selected gelator NDC-NN3 (20 mg mL^{-1}) were carried out. The results indicated that PDA-N4 could form supramolecular gels in mixed solvents of ethanol and water at low water fraction (less than or equal to 5%), and no gelation was observed when water fraction greater than or equal to 10%. These results reveal that solvents can notably involve in the gelation process, and the gelation property could be influenced by solvent polarity.

In order to obtain insights into the relationship between the chemical structure and the ultrasound induced gelation properties, the sonogelation behaviors of some structurally related compounds, NDC-NN4, NDC-NN2, NDC-NNpH, NDC-N4 and NDC-N3, were also inspected. No gelation was observed for all organic mediums selected for the experiments (Table S1 and S2†). These results imply that the gelling abilities of the gelator strongly depend on their molecular structures. The minor change of the molecular structure will make the gelator lose its gelling ability.

3.2 Rheological properties

To explore the mechanical properties of the sonogels, rheological measurements of NDC-NN3 gels formed in various organic mediums (such as ethanol, tetrahydrofuran and 1,4-dioxane) were performed. As shown in Fig. 2, the storage modulus (G') and loss modulus (G'') are independent of the stress below a critical strain region, suggesting that the gel structure keeps completely intact. When the stress is applied beyond a certain level, a disruption of the gels occurs, as demonstrated by a steep drop in the values of both moduli and the reversal of viscoelastic signals. Furthermore, the frequency sweep from 0.1 to 100 rad s^{-1} demonstrates a typical rheogram of gel, with $G' > G''$ over the whole frequency range. Additionally, the variation tendency of the G' and G'' of sonogels (formed from ethanol and 1,4-dioxane, 10 mg mL^{-1}) with increasing temperature was investigated. As depicted in Fig. S11 (ESI),† both moduli values of NDC-NN3 sonogels almost keep constant at low temperature, but decrease rapidly over the gel–sol transition temperatures (T_{g-s}) in which G' equals to G'', and finally G'' exceeds to G', indicating the gradual transformation from gel to solution. The T_{g-s} of sonogels (10 mg mL^{-1}) formed from ethanol and 1,4-dioxane is 67 and 78 °C, respectively, indicating that the sonogel of 1,4-dioxane is more thermostable than ethanol sonogel.

3.3 Morphology and microstructure

Solvent properties not only affect gelation abilities, but also play a pivotal role in mediating the self-assembly of molecules.[14] As a consequence, the influence of solvent properties on sonogel morphology was also explored by SEM. As shown in Fig. 3, the aggregates of NDC-NN3 in sonogels prepared from different
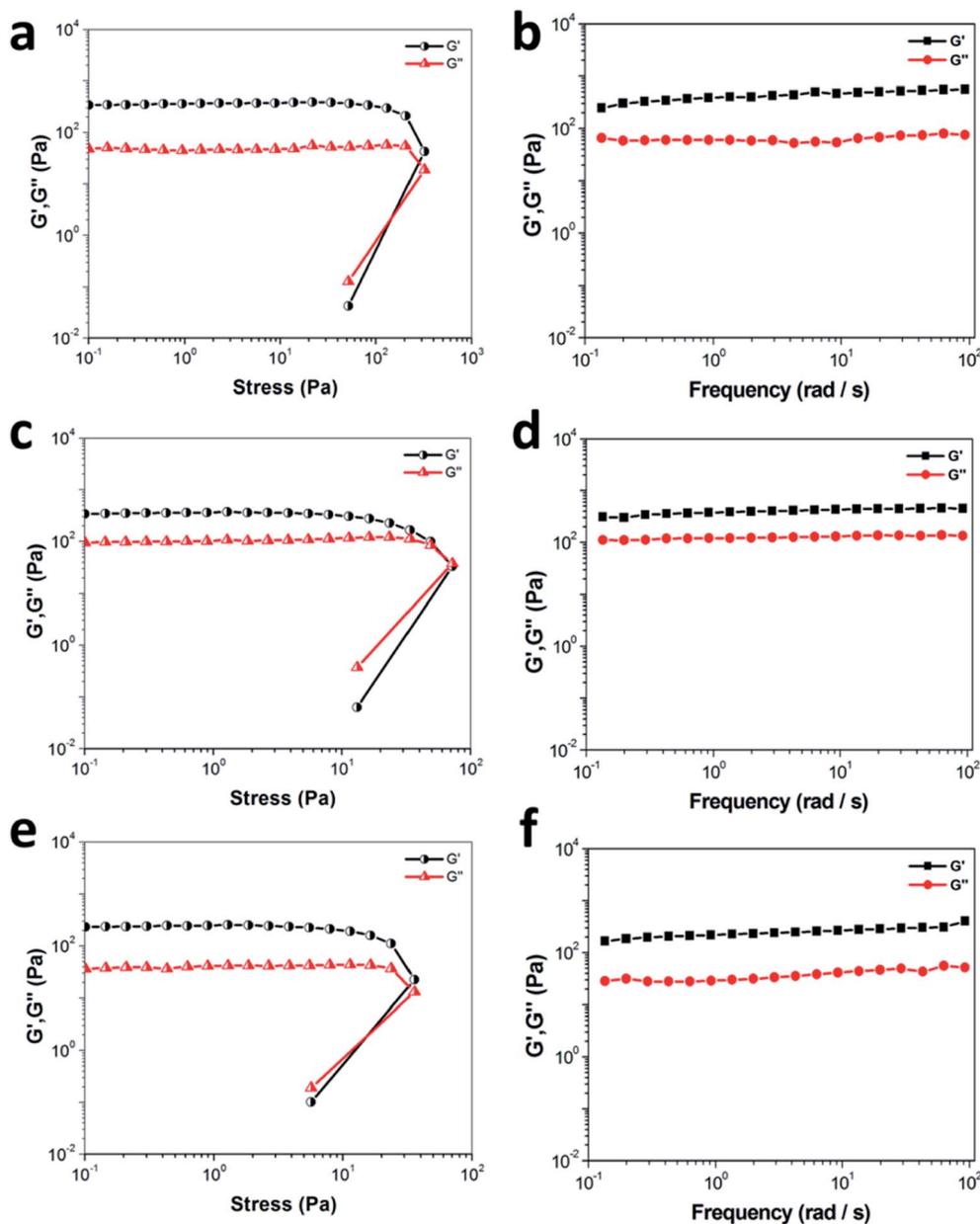
Fig. 2 Rheological behavior of NDC–NN3 sonogels (10 mg mL^{-1}) formed in ethanol, THF and 1,4-dioxane, respectively: (a, c and e) strain sweep modes; (b, d and f) frequency sweep modes at a constant stress of 5Pa.

solvents display a variety of forms. In ethanol, NDC-NN3 self-assembles into an intertwined 3D network consisting of 1D nanofibrers with the diameter of 200–800 nm. However, the sonogel prepared from tetrahydrofuran exhibits crumpled sphere-like morphology with the diameter of 1–3μm. The sonogel of 1,4-dioxane possesses a micro-burdockshaped balls structure with the diameter of 3–5μm consisting of thin twisted sheet. In addition, the fibrillar morphologies of sonogels formed in *n*-propanol, *n*-butanol and *n*-pentanol were observed (Fig. S12, ESI†). These results reveal that organic solvents can notably involve in the gelation process, as well as regulating the structure and properties of the sonogels.

3.4 Self-assembly mechanism

In experiments, it was found that the sonogels formed from NDC-NN3 in ethanol gradually transformed into pale yellow granular crystals upon extension of the aging time (Fig. S13, ESI†). As the concentration of NDC-NN3 increases, the duration for the transformation from gel to crystal decreases (Table S4, ESI†). In order to get insight into the transformation in detail, the gel–crystal transition process of NDC-NN3 sonogel formed in ethanol (20 mg mL^{-1}) was investigated by SEM and SA-XRD with the aging time prolonged to more than 30 days. As evidenced in Fig. S13a (ESI),† the xerogel prepared from the corresponding sonogel, which was aged at room temperature for
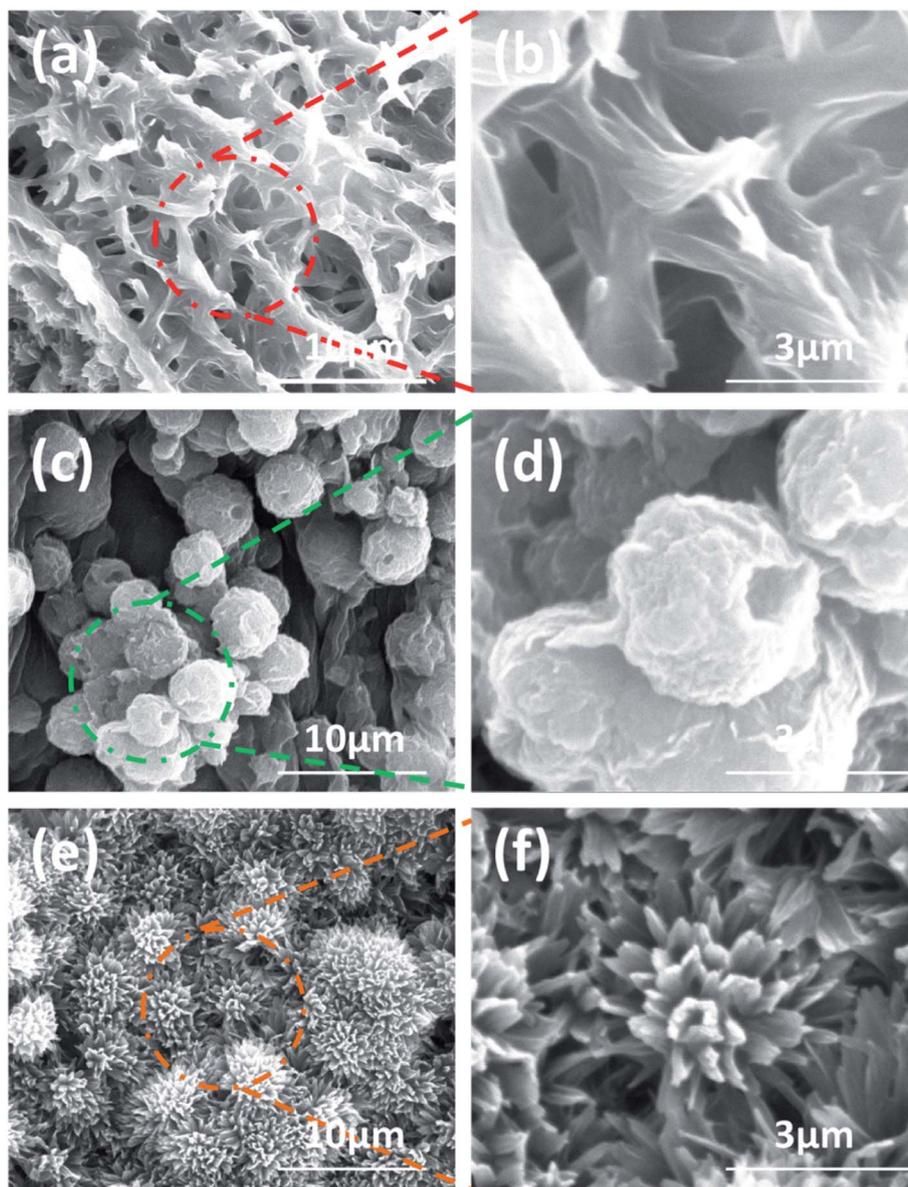
Fig. 3 SEM images of NDC-NN3 aggregates in dried sonogels formed in different solvents: (a and b) ethanol; (c and d) tetrahydrofuran; (e and f) 1,4-dioxane.

less than 5 days, is consisted of entangled fibers with the diameter of 200–800 nm. When the aging time is extended to 10 days, some granular crystals appear while the entangled fibers dissolution (Fig. S13b, ESI†). The appearance of crystals made the fibrous network less effective to immobilize the solvent, leading to the gradual destruction of gels. When the as-prepared sonogel is aged for 30 days, bulk crystals are generated (Fig. S13c, ESI†). The corresponding SA-XRD patterns of the sonogel for different aging time at 25 °C are presented in Fig. S14 (ESI).† Three prominent broad diffraction peaks at 8.4°, 16.7° and 24.2° for aerogel are observed (Fig. S14a, ESI†). However, the sonogel slowly transforms into granular crystal with prolonging ageing time, and some new sharp diffraction peaks occurs (Fig. S14b, ESI†). When the aging time is extended to 30 days, the three diffraction peaks attributed to sonogels are

disappeared, only the sharp diffraction peaks of crystals observed (Fig. S14c, ESI†). This phenomenon suggests that the sonogel should be a kinetic product and tend to form more stable thermodynamic crystals upon aging for a certain time. Similar results were also observed in previous reports.[15]

In order to understand how molecules self-assemble into crystals and the relationship between gelation and crystallization, single-crystal structure of NDC-NN3 in the sonogel with ethanol as solvent was investigated. The crystal data, selected bond lengths and angles are listed in Table S5 and S6 (ESI),† respectively. Further structure information has been deposited at the Cambridge Crystallographic Data Centre (CCDC 2031627). As showed in Fig. 4a, the crystal is composed of NDC-NN3 and solvent molecules, which are connected by intermolecular interactions including π–π stacking and hydrogen

bonding. The hydrogen bonding exists in neighbouring NDC-NN3 molecules, as well as the adjacent NDC-NN3 and solvent molecules. Comparing the SA-XRD pattern of NDC-NN3 xerogel with that of its crystal, the total difference of their diffraction peaks reveals that NDC-NN3 adopts different packing mode. The well-defined SA-XRD pattern of NDC-NN3 xerogel displays the d-spacing of 1.0514, 0.5306 and 0.3673 nm (related $2\theta =$ 8.4°, 16.7° and 24.2°), calculated from Bragg's equation, corresponding to the ratio of 1 : 1, 1 : 2 and 1 : 3, respectively. This result indicates that the sonogelator molecule self-assembles into a lamellar structure with a d-spacing of 1.0514 nm (Fig. S14a, ESI†).[16] The long d-spacing (D) (1.0514 nm) is much smaller than the length of NDC-NN3 molecular (2.1396 nm, Fig. S15, ESI†) evaluated by the Corey–Pauling–Koltun (CPK) space-filling model, demonstrating that NDC-NN3 molecules

adopt a packing mode with the molecular plane highly tilted to the lamellar normal.[17]

To further explore the self-assembly mechanism, FT-IR and variable-time ^{1}H NMR spectra were collected. As illustrated in Fig. S16 (ESI),† the FT-IR spectra of NDC-NN3 crystal and aerogels formed in different solvents are all characterized by vibration bands appearing at *ca.* 1657 and 3234 cm^{-1}, which could be attributed to the C=O and N–H stretching vibrations of intermolecular hydrogen bonds for hydrazide, respectively. This phenomenon reveals that the intermolecular hydrogen bonding interactions formed in neighboring gelator molecules exist in both NDC-NN3 aerogel and crystal. Similar result has been proved in crystal structure of NDC-NN3 (*vide supra*). Fig. S17 (ESI)† displays the variable-time ^{1}H NMR spectra of NDC-NN3 sonogel (ethanol-d$_6$, 20 mg mL^{-1}). It can be found that the sharp aromatic proton signals of NDC-NN3 in solution
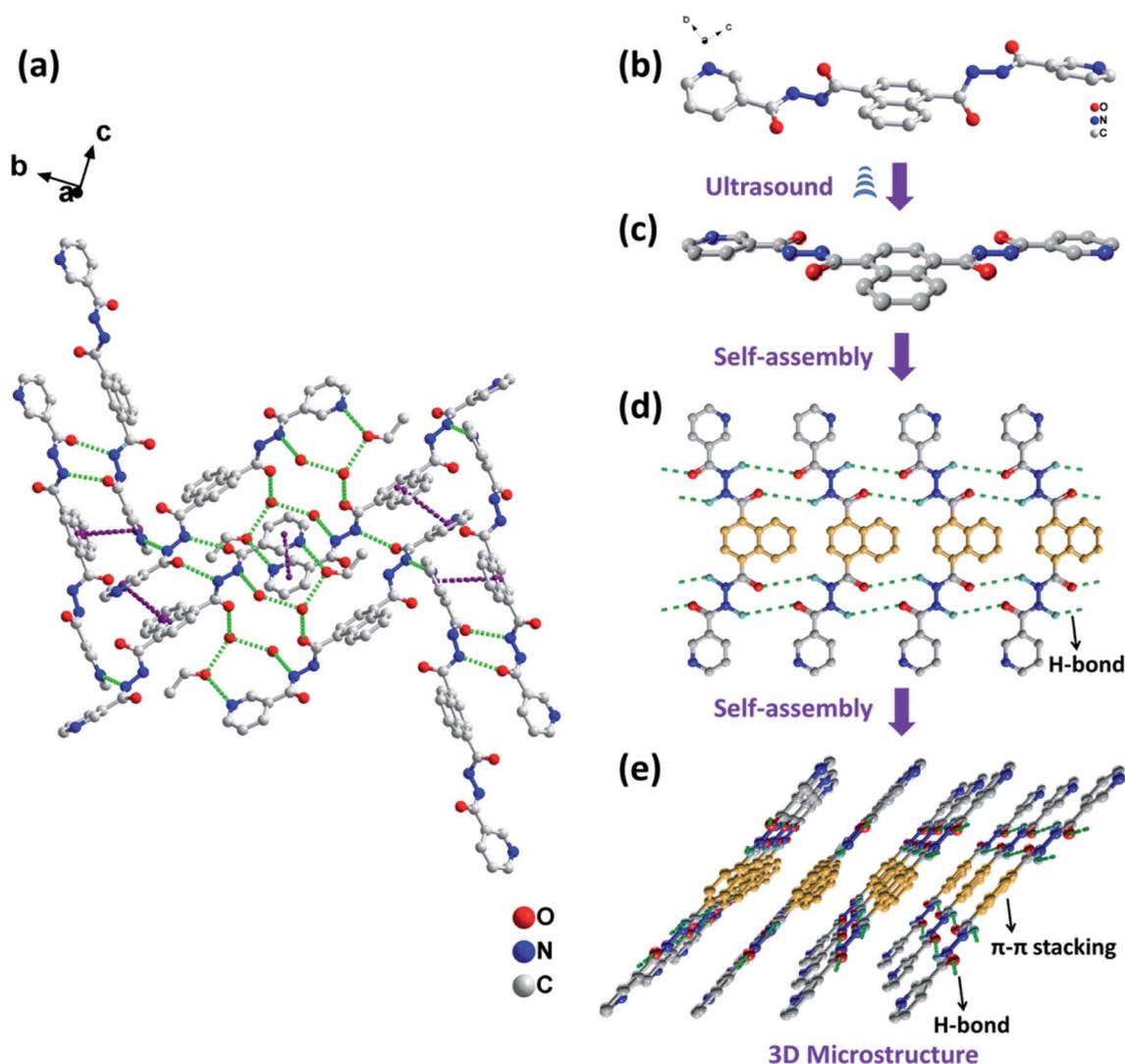

Fig. 4 Intermolecular interactions that exist in NDC-NN3 crystals (green and purple dashed lines indicate hydrogen bonds and π–π stacking interactions, respectively). (a) Single crystals structure of NDC-NN3; (b) structure of NDC-NN3 molecule adopt a conformation of the lowest energy in solution; (c) metastable planar conformation of NDC-NN3; (d) supramolecular aggregates of NDC-NN3 formed from the metastable planar conformation; (e) in the gel of NDC-NN3, the aggregate consists of repeating lamellar units, which adopt the molecular plane highly tilted to the lamellar normal.
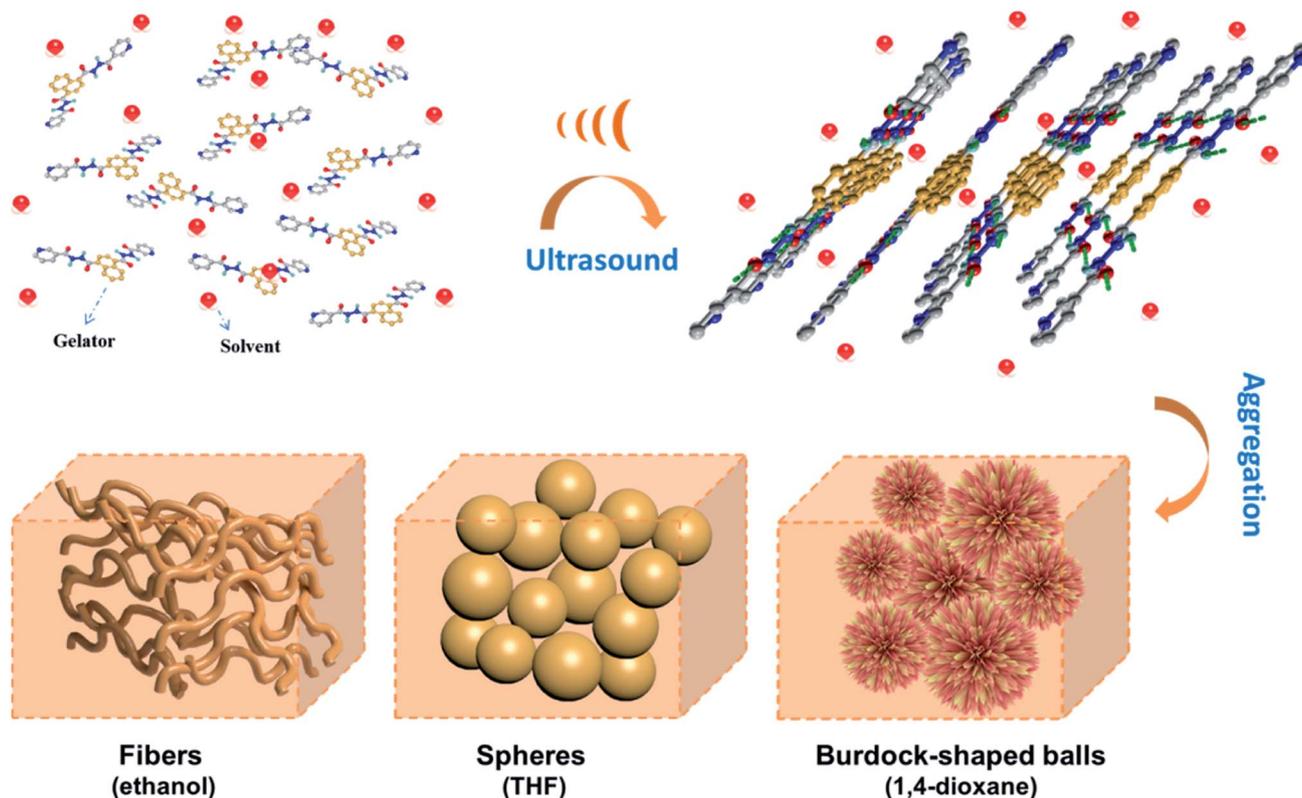
Fibers (ethanol)

Spheres (THF)

Burdock-shaped balls (1,4-dioxane)

Fig. 5 Schematic representation of the possible self-assembly mechanism of NDC–NN3 sonogel.

phase appear at 9.16 (d, H_a), 8.82 (dd, H_b), 8.49 (dd, H_c), 8.39–8.30 (m, H_d), 7.79 (s, H_e), 7.76–7.69 (m, H_f), 7.67–7.59 ppm (m, H_g). With the sonication time increasing to 30 min, they become gradually widened and the corresponding intensity extraordinarily decreases, indicating that NDC–NN3 molecules are incorporated into the gel, and thus the motion is restricted, rendering it more solid-like.[9b] The up-field shifts of the aromatic proton signals upon sonication suggest that π–π stacking interactions have been gradually formed in the new phase. In fact, a stable sonogel is formed after sonication for 30 min.

Based on these results, it can be deduced that the NDC-NN3 molecules adopt a conformation of the lowest energy in solution as illustrated in the single crystals structure (Fig. 4b). When the solution of NDC-NN3 is irradiated by sonication, the NDC-NN3 molecules gradually tend to form a metastable planar conformation (Fig. 4c) which has been proved by the results of NMR and XRD experiments. The metastable planar conformation promotes the NDC-NN3 molecules to form supramolecular aggregates (Fig. 4d) which render their solubility decrease and then form a stable sonogel finally. In the gel, the aggregate consists of repeating lamellar units, which adopt the molecular plane highly tilted to the lamellar normal (Fig. 4e and S18, ESI†). Within the lamellar unit, adjacent organogelator molecules are linked by intermolecular hydrogen bonds and π–π stacking interactions to form a hydrogen-bonding network. The lamellar unit further assembles into fibers, spheres or micro-burdockshaped balls and thus creates a three-dimensional (3D) network, in which abundant liquid is immobilized in the

interspaces, resulting in the formation of supramolecular sonogel as illustrated in Fig. 5.

4. Conclusion

In summary, we have designed and synthesized a new type of hydrazide derivatives, NDC-NN3, which could form gels in some organic liquids induced by sonication. In the as-obtained sonogels for different solvents, the gelators self-assemble into fibers, spheres and micro-burdockshaped balls. They display excellent mechanical properties and are kinetic products. The crystal structure of NDC-NN3 suggests that the naphthalene ring, hydrazide group and the position of N in pyridine ring mediate the self-assembly process. Upon sonication, the formation of suitable π–π stacking and intermolecular hydrogen bonding drives gelator molecules self-assembly and the final gelation. Overall, this study illustrates the importance of the structure–sonogelation relationship and provides new insights into the design of smart soft materials.

Conflicts of interest

There are no conflicts of interest to declare.

Acknowledgements

References

1 (a) S. K. Mellerup and S. N. Wang, *Chem. Soc. Rev.*, 2019, **48**, 3537–3549; (b) E. R. Ruskowitz and C. A. DeForest, *Nat. Rev. Mater.*, 2018, **3**, 17087; (c) P. Sutara and T. K. Maji, *Chem. Commun.*, 2016, **52**, 8055–8074; (d) A. J. McConnell, C. S. Wood, P. P. Neelakandan and J. R. Nitschke, *Chem. Rev.*, 2015, **115**, 7729–7793; (e) P. Theato, B. S. Sumerlin, R. K. O'Reilly and T. H. Epps III, *Chem. Soc. Rev.*, 2013, **42**, 7055–7056.

2 (a) A. C. Daly, L. Riley, T. Segura and J. A. Burdick, *Nat. Rev. Mater.*, 2020, **5**, 20–43; (b) H. Ke, L. P. Yang, M. Xie, Z. Chen, H. Yao and W. Jiang, *Nat. Chem.*, 2019, **11**, 470–477; (c) E. R. Draper and D. J. Adams, *Chem. Soc. Rev.*, 2018, **47**, 3395–3405; (d) B. O. Okesola and D. K. Smith, *Chem. Soc. Rev.*, 2016, **45**, 4226–4251; (e) J. Boekhoven, W. E. Hendriksen, G. J. M. Koper, R. Eelkema and J. H. van Esch, *Science*, 2015, **349**, 1075–1079; (f) D. C. Zhong, L. Q. Liao, K. J. Wang, H. J. Liu and X. Z. Luo, *Soft Matter*, 2015, **11**, 6386–6392; (g) J. W. Steed, *Chem. Commun.*, 2011, **47**, 1379–1383; (h) N. M. Sangeetha and U. Maitra, *Chem. Soc. Rev.*, 2005, **34**, 821–836.

3 (a) R. Kuosmanen, K. Rissanen and E. S. ievanen, *Chem. Soc. Rev.*, 2020, **49**, 1977–1998; (b) P. R. A. Chivers and D. K. Smith, *Nat. Rev. Mater.*, 2019, **4**, 463–478; (c) E. R. Draper and D. J. Adams, *Chem. Commun.*, 2016, **52**, 8196–8206; (d) X. D. Yu, L. M. Chen, M. M. Zhang and T. Yi, *Chem. Soc. Rev.*, 2014, **43**, 5346–5371; (e) M. D. Segarra-Maset, V. J. Nebot, J. F. Miravet and B. Escuder, *Chem. Soc. Rev.*, 2013, **42**, 7086–7098; (f) M. O. M. Piepenbrock, G. O. Lloyd, N. Clarke and J. W. Steed, *Chem. Rev.*, 2010, **110**, 1960–2004; (g) J. A. Foster, M. M. Piepenbrock, G. O. Lloyd, N. Clarke, J. A. K. Howard and J. W. Steed, *Nat. Chem.*, 2010, **2**, 1037–1043.

4 T. Naota and H. Koori, *J. Am. Chem. Soc.*, 2005, **127**, 9324–9325.

5 (a) N. Komiya, T. Muraoka, M. Lida, M. Miyanaga, T. Talahashi and T. Naota, *J. Am. Chem. Soc.*, 2011, **133**, 16054–16061; (b) K. Isozaki, H. Takaya and T. Naota, *Angew. Chem., Int. Ed.*, 2007, **46**, 2855–2857.

6 (a) R. Afrasiabi and H. Kraatz, *Chem.– Eur. J.*, 2013, **19**, 1769–1777; (b) D. Ke, C. Zhan, A. D. Q. Li and J. Yao, *Angew. Chem., Int. Ed.*, 2011, **50**, 3715–3719; (c) D. Bardelang, F. Camerel, J. C. Margeson, D. Leek, M. Schmutz, M. B. Zaman, K. Yu, D. V. Soldatov, R. Ziessel, C. I. Ratcliffe and J. A. Ripmeester, *J. Am. Chem. Soc.*, 2008, **130**, 3313–3315.

7 (a) J. T. V. Herpt, M. C. A. Stuart, W. R. Browne and B. L. Feringa, *Langmuir*, 2013, **29**, 8763–8767; (b) C. Wang, D. Zhang and D. Zhu, *J. Am. Chem. Soc.*, 2005, **127**, 16372–16373.

8 (a) X. D. Yu, Q. Liu, J. C. Wu, M. Zhang, X. Cao, S. Zhang, Q. Wang, L. Chen and T. Yi, *Chem.– Eur. J.*, 2010, **16**, 9099–9106; (b) J. Wu, T. Yi, T. Shu, M. Yu, Z. Zhou, M. Xu, Y. Zhou, H. Zhang, J. Han, F. Li and C. Huang, *Angew. Chem., Int. Ed.*, 2008, **47**, 1063–1067.

9 (a) K. M. Anderson, G. M. Day, M. J. Paterson, P. Byrne, N. Clarke and J. W. Steed, *Angew. Chem., Int. Ed.*, 2008, **47**, 1058–1062; (b) D. Nunez-Villanueva, M. A. Jinks, J. Gomez Magenti and C. A. Hunter, *Chem. Commun.*, 2018, **54**, 10874–10877.

10 (a) C. D. Jones and J. W. Steed, *Chem. Soc. Rev.*, 2016, **45**, 6546–6596; (b) D. Bardelang, M. Z. Zaman, I. L. Moudrakovski, S. Pawsey, J. C. Margeson, D. Wang, X. Wu, J. A. Ripmeester, C. I. Ratcliffe and K. Yu, *Adv. Mater.*, 2008, **20**, 4517–4520; (c) X. Wang, J. A. Kluge, G. G. Leisk and D. L. Kaplan, *Biomaterials*, 2008, **29**, 1054–1064; (d) J. M. J. Paulusse and R. P. Sijbesma, *Angew. Chem., Int. Ed.*, 2006, **45**, 2334–2337; (e) D. R. Trivedi and P. Dastidar, *Chem. Mater.*, 2006, **18**, 1470–1478.

11 (a) A. Y. Dang-i, T. Huang, N. Mehwish, X. Dou, L. Yang, V. Mukwaya, C. Xing, S. Lin and C. L. Feng, *ACS Appl. Bio Mater.*, 2020, **3**, 2295; (b) Ł. Popiołek, *Med. Chem. Res.*, 2017, **26**, 287–301.

12 (a) D. H. Wu, J. T. Song, L. Qu, W. L. Zhou, L. Wang, X. G. Zhou and H. F. Xiang, *Chem.–Asian J.*, 2020, **15**, 1–10; (b) S. J. Beckers, S. Parkinson, E. Wheeldon and D. K. Smith, *Chem. Commun.*, 2019, **55**, 1947–1950; (c) T. Zhang, X. Che, C. Zhang, B. Bai, H. Wang and M. Li, *Soft Mater.*, 2019, **17**, 383–390; (d) L. He, X. Ran, J. Li, Q. Gao, Y. Kuang and L. Guo, *J. Mater. Chem. A*, 2018, **6**, 16600–16609; (e) S. Lu, J. Huang, G. T. Liu, Z. Lin, Y. Li, X. Huang, C. Huang and S. Wu, *RSC Adv.*, 2017, 7, 30979–30983; (f) C. Zhang, T. Zhang, N. Ji, Y. Zhang, B. Bai, H. Wang and M. Li, *Soft Matter*, 2016, **12**, 1525–1533; (g) Y. Li, X. Ran, Q. Li, Q. Gao and L. Guo, *Chem.–Asian J.*, 2016, **11**, 2157–2166; (h) P. Malakar and E. Prasad, *Chem. – Eur. J.*, 2015, **21**, 1–9; (i) M. Bielejewski, J. Kowalczuk, J. Kaszyńska, A. Łapiński, R. Luboradzki, O. Demchuk and J. Tritt-Goc, *Soft Matter*, 2013, **9**, 7501–7514; (j) L. Y. You, G. T. Wang, X. K. Jiang and Z. T. Li, *Tetrahedron*, 2009, **65**, 9494–9504; (k) G. Cravotto and P. Cintas, *Chem. Soc. Rev.*, 2009, **38**, 2684–2697; (l) Y. Yang, T. Chen, J. F. Xiang, H. J. Yan, C. F. Chen and L. J. Wan, *Chem. – Eur. J.*, 2008, **14**, 5742–5746; (m) Y. Yang, H. J. Yan, C. F. Chen and L. J. Wan, *Org. Lett.*, 2007, **9**(24), 4991l–4994; (n) N. Sreenivasachary and J. M. Lehn, *Proc. Natl. Acad. Sci. U. S. A.*, 2005, **102**, 5938–5943.

13 (a) J. W. Liu, J. T. Ma and C. F. Chen, *Tetrahedron*, 2011, **67**, 85–91; (b) Y. Zhang, H. Ding, Y. Wu, C. Zhang, B. Bai, H. Wang and M. Li, *Soft Matter*, 2014, **10**, 8838–8845.

14 (a) G. Yang, C. Lin, X. Feng, T. Wang and J. Jiang, *Chem. Commun.*, 2020, **56**, 527–530; (b) L. Q. Liao, X. Zhong, X. J. Jia, C. Y. Liao, J. L. Zhong, S. M. Ding, C. Chen,

S. G. Hong and X. Z. Luo, *RSC Adv.*, 2020, **10**, 29129–29138; (*c*) S. Xue, P. Xing, J. Zhang, Y. Zeng and Y. Zhao, *Chem.– Eur. J.*, 2019, **25**, 7426–7437; (*d*) Y. Lan, M. G. Corradini, R. G. Weiss, S. R. Raghavanc and M. A. Rogers, *Chem. Soc. Rev.*, 2015, **44**, 6035–6058.

15 (*a*) T. Guterman, M. Levin, S. Kolusheva, D. Levy, N. Noor, Y. Roichman and E. Gazit, *Angew. Chem., Int. Ed.*, 2019, **58**, 15869–15875; (*b*) X. Jia, J. Wang, D. Zhong, J. Wu, B. Zhao, D. den Engelsena and X. Luo, *RSC Adv.*, 2016, **6**, 109425–

109433; (*c*) D. K. Kumar and J. W. Steed, *Chem. Soc. Rev.*, 2014, **43**, 2080–2088.

16 (*a*) I. W. Hamley and V. Castelletto, *Prog. Polym. Sci.*, 2004, **29**, 909–948; (*b*) M. Deng, L. Zhang, Y. Jiang and M. Liu, *Angew. Chem., Int. Ed.*, 2016, **55**, 1–6.

17 (*a*) X. Luo, Z. Li, W. Xiao, Q. Wang and J. Zhong, *J. Colloid Interface Sci.*, 2009, **336**, 803–807; (*b*) D. J. Cram, *Science*, 1988, **240**, 760–767.